Raman-assisted Brillouin optical time-domain analysis with sub-meter resolution over 100 km

X. Angulo-Vinuesa,[1,*] S. Martin-Lopez,[1] P. Corredera,[1] and M. Gonzalez-Herraez[2]

[1]*Instituto de Óptica, Consejo Superior de Investigaciones Científicas (CSIC), 28006 Madrid, Spain*
[2]*Departamento de Electrónica, Universidad de Alcalá, 28871 Alcalá de Henares, Madrid, Spain*
**xabier.angulo@io.cfmac.csic.es*

Abstract: Sub-meter resolution in long-distance Brillouin Optical Time Domain Analysis (BOTDA) cannot be trivially achieved due to several issues including: resolution-uncertainty trade-offs, self-phase modulation, fiber attenuation, depletion, etc. In this paper we show that combining Raman assistance, differential pulse-width pair (DPP) measurements and a novel numerical de-noising procedure, we could obtain sub-meter resolution Brillouin optical time-domain analysis over a range of 100 km. We successfully demonstrate the detection of a 0.5 meter hot-spot in the position of worst contrast along the fiber.

OCIS codes: (290.5900) Scattering, stimulated Brillouin; (060.2370) Fiber optics sensors; (290.5910) Scattering, Raman.

References and links

1. T. Horiguchi and M. Tateda, "Optical-fiber-attenuation investigation using stimulated Brillouin scattering between a pulse and a continuous wave," Opt. Lett. **14**(8), 408–410 (1989).
2. T. Horiguchi and M. Tateda, "BOTDA – nondestructive measurement of single-mode optical fiber attenuation characteristics using Brillouin interaction: theory," J. Lightwave Technol. **7**(8), 1170–1176 (1989).
3. G. P. Agrawal, *Nonlinear Fiber Optics* (Academic, 2007).
4. A. Minardo, R. Bernini, and L. Zeni, "Stimulated Brillouin scattering modeling for high-resolution, time-domain distributed sensing," Opt. Express **15**(16), 10397–10407 (2007).
5. H. Naruse and M. Tateda, "Trade-off between the spatial and the frequency resolutions in measuring the power spectrum of the Brillouin backscattered light in an optical fiber," Appl. Opt. **38**(31), 6516–6521 (1999).
6. S. M. Foaleng, F. Rodríguez-Barrios, S. Martin-Lopez, M. González-Herráez, and L. Thévenaz, "Detrimental effect of self-phase modulation on the performance of Brillouin distributed fiber sensors," Opt. Lett. **36**(2), 97–99 (2011).
7. W. Li, X. Bao, Y. Li, and L. Chen, "Differential pulse-width pair BOTDA for high spatial resolution sensing," Opt. Express **16**(26), 21616–21625 (2008).
8. F. Rodriguez-Barrios, S. Martin-Lopez, A. Carrasco-Sanz, P. Corredera, J. D. Ania-Castañón, L. Thévenaz, and M. Gonzalez-Herraez, "Distributed Brillouin fiber sensor assisted by first-order Raman amplification," J. Lightwave Technol. **28**(15), 2162–2172 (2010).
9. X. Angulo-Vinuesa, S. Martin-Lopez, J. Nuno, P. Corredera, J. D. Ania-Castañón, L. Thévenaz, and M. Gonzalez-Herraez, "Raman assisted Brillouin distributed temperature sensor over 100 km featuring 2 m resolution and 1.2 °C uncertainty," J. Lightwave Technol. **30**(8), 1060–1065 (2012).
10. M. A. Soto, G. Bolognini, and F. Di Pasquale, "Optimization of long-range BOTDA sensors with high resolution using first-order bi-directional Raman amplification," Opt. Express **19**(5), 4444–4457 (2011), http://8.18.37.105/oe/viewmedia.cfm?uri=oe-19-5-4444&seq=0.
11. M. J. Conelly, *Semiconductor Optical Amplifiers* (Kluwer Academic Press, 2002).
12. A. Minardo, R. Bernini, and L. Zeni, "Numerical analysis of single pulse and differential pulse-width pair BOTDA systems in the high spatial resolution regime," Opt. Express **19**(20), 19233–19244 (2011).
13. L. Thévenaz, S. Foaleng Mafang, and J. Lin, "Impact of pump depletion on the determination of the Brillouin gain frequency in distributed fiber sensors," Proc. SPIE **7753**, 775322 (2011).
14. M. Niklés, L. Thévenaz, and P. A. Robert, "Brillouin gain spectrum characterization in single-mode optical fibers," J. Lightwave Technol. **15**(10), 1842–1851 (1997).

1. Introduction

Brillouin Optical Time Domain Analysis (BOTDA) [1–2] allows distributed measurements of temperature and strain over conventional Single Mode Fibers (SMF). The necessary physical phenomenon to develop a BOTDA is the nonlinear optical effect denominated Stimulated Brillouin Scattering (SBS) [3]. SBS produces a counter-propagating narrowband

#165389 - $15.00 USD Received 23 Mar 2012; revised 27 Apr 2012; accepted 28 Apr 2012; published 14 May 2012

amplification of a probe signal within the fiber when an intense coherent pump light is introduced through one of the ends of the SMF. Distributed measurements are made possible by pulsing the pump signal and measuring the probe signal variation as a function of the time-of-flight of the pump pulse within the fiber.

The spatial resolution of the BOTDA, therefore, comes determined by the length of the pulses employed as a pump signal (roughly 1 meter per 10 ns). Shorter pulses lead to higher resolutions; however this approach has an intrinsic limitation in uncertainty. The reason comes from the fact that the observed Brillouin gain spectrum broadens for shorter pulses [4]. This broadening leads to larger uncertainties in the determination of the Brillouin shift. A natural limit can be found when pump pulse and natural Brillouin gain spectra show comparable bandwidths, corresponding to pump pulses with duration of ~10 ns, or ~1 meter. This is known as the resolution-uncertainty trade-off [5]. In long-range systems, this trade-off is worsened by the additional detrimental effect of self-phase modulation, which introduces an extra spectral broadening of the pulses as they travel along the fiber [6].

To avoid the inevitable physical limitations associated to pump pulse shortening in high-resolution setups, the Differential Pulse-width Pair (DPP) technique has been proposed [7]. This technique allows increasing the resolution of BOTDA fiber sensors without broadening the gain spectrum and avoiding self-phase modulation issues. It bases its working principle in the subtraction between gain traces obtained with slightly different pulse widths. The spatial resolution is then given by the differential width between the pulses while the broadening in the gain remains bounded since the pulses used are always much longer than the phonon lifetime (typically 4-6 times larger). The effect of self-phase modulation in these schemes should also be residual for the typical power levels used.

Conventional BOTDA configurations also show limitations in terms of working range. The fiber attenuation inevitably reduces the gain along the fiber, leading to a contrast loss and an increase in uncertainty in the far end. Long-range (beyond 60 km) measurements in BOTDA sensors are preferably achieved with the help of a faint distributed amplification along the sensing fiber, typically achieved through the use of stimulated Raman gain [8]. Raman assistance provides a good way of maintaining the power level of the pump pulse along the fiber, and hence the Brillouin gain contrast achieved. However, it also has inevitable limitations, namely related to the Relative Intensity Noise (RIN) transfer from the Raman pumps to the Brillouin probe [8]. To the best of our knowledge, the best resolution demonstrated so far in sensors with ≥100 km range has been in the order of 2 meters [9–10]. While this performance is enough for most applications, extending the resolution to sub-meter values in Raman-assisted configurations is also desirable.

In this work, we employ the DPP technique and a novel RIN de-noising technique in a long-range Raman-assisted Brillouin distributed sensor. We demonstrate, for the first time to our knowledge, the possibility of achieving sub-meter resolution in a 100 km range sensor.

2. Experimental setup and RIN de-noising procedure

The experimental setup is depicted in Fig. 1. It is very similar to the Raman-assisted BOTDA scheme described in [9], except for a couple of differences. The first difference comes from the fact that the element that makes the pump pulse is a Semiconductor Optical Amplifier (SOA) instead of an Electro-Optic Modulator (EOM) and a Nonlinear Optical Loop Mirror (NOLM). This makes the setup easier to operate while the extinction ratio remains very high (>50 dB) [11]. It also allows reducing one amplification stage in the pump branch, which improves slightly the signal-to-noise ratio. In addition, the high extinction ratio of these pulses helps to improve the spectral purity in the measurements done with the DPP configuration, as shown in the numerical results of Minardo et al. [12].

#165389 - $15.00 USD Received 23 Mar 2012; revised 27 Apr 2012; accepted 28 Apr 2012; published 14 May 2012

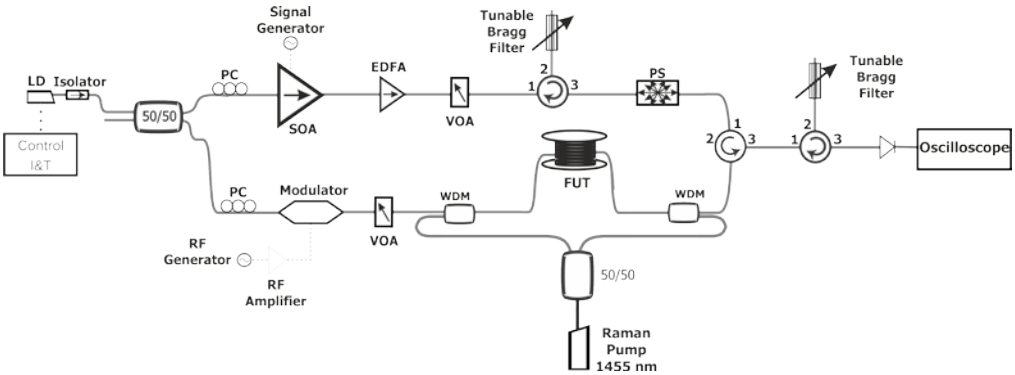

Fig. 1. Experimental setup of the Raman-assisted distributed sub-meter Brillouin sensor. LD: Laser Diode; PC: Polarization Controller; SOA: Semiconductor Optical Amplifier; EDFA: Erbium Doped Fiber Amplifier; VOA: Variable Optical Attenuator; WDM: Wavelength Division Multiplexer; FUT: Fiber Under Test; PS: Polarization Scrambler.

The second difference comes from the use of a shorter wavelength laser (the present laser has the central wavelength at 1548.5 nm, shorter than the laser used in [9]). In essence this does not have any impact on the experiment except that the filtering in detection is also shifted and the Brillouin shift curve is up-shifted with respect to the values reported in [9] for the same fiber spools.

Another key difference with respect to the setup described in [9] lies in the de-noising procedure that has been put forward to eliminate as much as possible the effect of RIN transfer from the Raman pump to the Brillouin probe. In previous implementations of Raman-assisted BOTDA, RIN transfer has been recognized as a major impairment, especially in the usual case of using Raman Fiber Lasers (RFLs) as Raman pumps [8–10]. For the purpose of minimizing the RIN contribution, it is important to realize that Raman Fiber Lasers show a spectrum composed of many modes with a periodic spacing. This periodic mode spacing (normally in the hundreds of kHz- few MHz range for typical RFLs) leads to the appearance of some quasi-periodic intensity perturbations which may not wash out even after the usual trace averaging procedure (in particular, when the mode spacing happens to be a multiple of the pump pulse repetition rate, see Fig. 2(a)). It is also remarkable that the frequency position of these periodic perturbations is not strictly fixed since the Raman laser cavity is long and thermal drifts may favor different mode beating frequencies. In our case, a digital filtering algorithm has been put forward to eliminate this quasi-periodic noise in the traces. The use of this algorithm is justified since, conventionally, these sensors are not made to detect any periodic strain or temperature variations. They are normally adapted to detect and measure hot-spots or particularly strained sections of short length (e.g. pipeline leaks, cracks in structures, etc.), or anyway non-periodic variations in the Brillouin shift. Sharp peaks in the trace spectra corresponding to periodic trace variations can therefore be safely detected and eliminated in the processing step without affecting the measurement results. As we will see, the results from the point of view of hot-spot detection are notably better with this simple procedure.

In our case, the procedure to remove the quasi-periodic noise in the trace has been implemented as follows: in the initial step, a Fast Fourier Transform (FFT) of the raw trace, and its preceding and succeeding traces in the frequency scan is performed. These spectra are averaged to obtain an “average” trace spectrum. Over this “average” spectrum, a peak search algorithm is applied, which detects the frequency positions showing a much larger energy over the four closest frequency bins. The threshold for this classification is established as 1% of the zero-frequency component of the FFT. These frequency positions (and their corresponding symmetric in the spectrum) are set to zero in the trace FFT. After this, the trace is recovered again through an inverse FFT. This procedure introduces an additional numerical noise in the trace. However this noise is very small, and the overall result is an improvement

#165389 - $15.00 USD Received 23 Mar 2012; revised 27 Apr 2012; accepted 28 Apr 2012; published 14 May 2012

of the signal quality. Furthermore, unlike other techniques, this procedure has no impact on the phase and therefore leaves the positional information of the trace fully preserved. An additional low-pass filtering at the cut-off frequency of the detector is done in the trace to ensure that any out-of-band noise in the acquisition is suppressed as much as possible.

Besides these novelties, the setup and the methodology to determine the adequate power settings are exactly the same as the ones employed previously in [9]. Differential measurements with 1 meter spatial resolution are obtained by subtracting the traces obtained with 65 and 55 ns pump pulses (0.8 and 0.5 meter resolution is obtained subtracting the traces obtained with 65 and 57 ns and 65 and 60 ns pump pulses respectively). In all cases, the fall times of the pump pulses, which are known to influence the resolution, are below 2 ns. With these settings, the pump fall time should not have a significant impact on the achievable resolution [12]. A simple normalization procedure ensures that the gain subtraction is robust against small pump power variations (the gain traces are normalized to their respective pulse widths). This procedure is correct as long as pump depletion effects can be considered negligible. In our case, the probe power is set below 90 μW, which in the case of symmetric sidebands in the probe, ensures no depletion, even for this very long length [13].

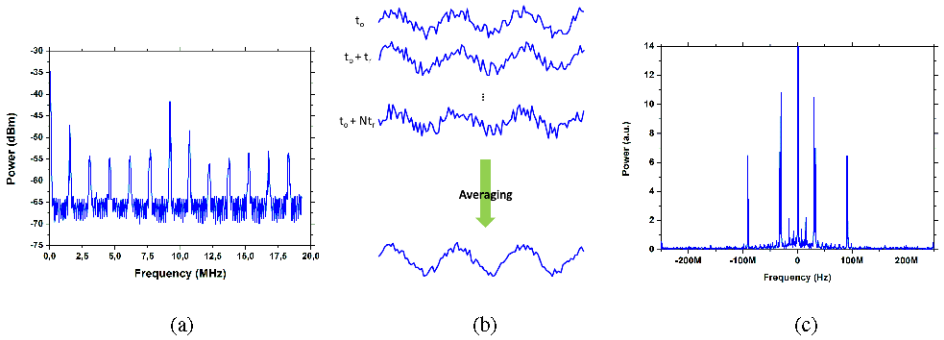

Fig. 2. Illustration of the effect of the RFL RIN transfer problem on the measurement and the strategy to avoid it. (a) Shows the intensity noise spectrum of the RFL used in the experiment, at the employed power values (500 mW). Since the RFL shows a chain of modes in the spectrum, its output displays some quasi-periodic intensity perturbations in multiple frequencies of the free spectral range of the laser. These quasi-periodic perturbations are transferred to the probe signal and may not be easily averaged out in the acquisition procedure if the acquisition trigger period is a multiple of the cavity round-trip time: 2(b). In the trace FFT spectrum, this effect appears as discrete "peaks" (see 2(c)) which can be easily removed with a digital filtering technique.

3. Results

In this section we will show the high-resolution results that we could obtain with the DPP Raman-assisted BOTDA. The 100 km fiber is composed by four SMF spools of 25 km with an effective area of 70 μm^2 and a similar Brillouin Frequency Shift (BFS) located at approximately 10.7 GHz for the laser wavelength (~1548.5 nm). The peak power of pump and probe were 6 mW and 81 μW respectively, with 500 mW of total Raman pump power (~250 mW per each side). In terms of Brillouin pump power, we could raise the power level to a value roughly 3 times higher than the values used in [9] for the 2 meter configuration over the same 100 km range. This is because the effect of self-phase modulation scales with the inverse of the pump pulse width. Since the pulses are 3 times longer, the power can be raised 3 times without adding extra spectral broadening. Combining the peak power increase and the pulse width increase, the gain values recorded in the experiments of this work are roughly 10 times larger than the ones recorded in [9]. The probe power is also increased with respect to the setup described in [9]. This obeys to a careful setting of the modulator working point to minimize the power imbalance between the two side-bands. With perfectly symmetric sidebands, the probe power can be theoretically raised up to a value close to the

#165389 - $15.00 USD Received 23 Mar 2012; revised 27 Apr 2012; accepted 28 Apr 2012; published 14 May 2012

SBS threshold without entering into undesired depletion problems. These changes lead to a >10 dB increase in trace SNR over the setup described in [9]. Figure 3 shows a gain trace recorded for the complete fiber length with a pulse width of 65 ns. The Raman pump power used is below the value necessary for a good compensation of the losses. However, this ensures a good behavior of the setup in terms of RIN transfer.

To validate the performance of our high-resolution long range BOTDA, even in the worst conditions, we introduce a hot spot between the last two fiber spools (around km 75), where the gain contrast is minimal. 1 meter of fiber was introduced in a water bath at 60°C (± 5°C), with a room temperature of 22°C. Figures 4(a) and 4(b) (65 and 55 ns pulses respectively) show the gain trace sweep around the hot-spot location for a probe frequency shift ranging from 10.66 GHz up to 10.78 GHz. As it can be seen, the BFS of the fiber is set at approximately 10.71 GHz all along the 100 meter span analyzed. At the hot spot region, it can be seen that the gain at 10.71 is reduced and a significant part of the gain is recorded at higher offset frequencies. The distance over which this change in gain behavior arises spans over the pulse length in both cases, being therefore longer for the gain sweep acquired with longer pulse length.

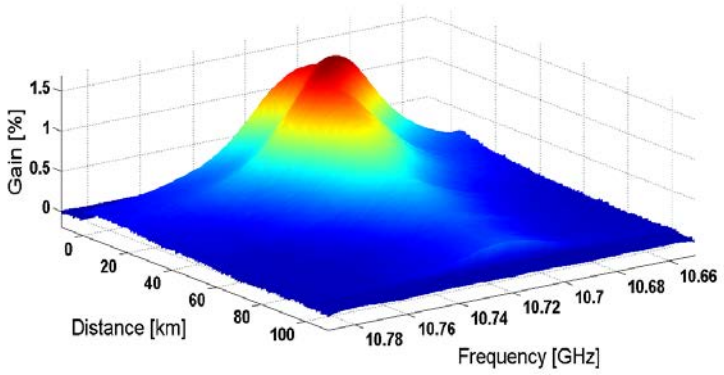

Fig. 3. Brillouin gain sweep for the complete fiber length. The probe signal frequency is swept from 10.66 GHz until 10.78 GHz and the traces are acquired with 65 ns pulses.

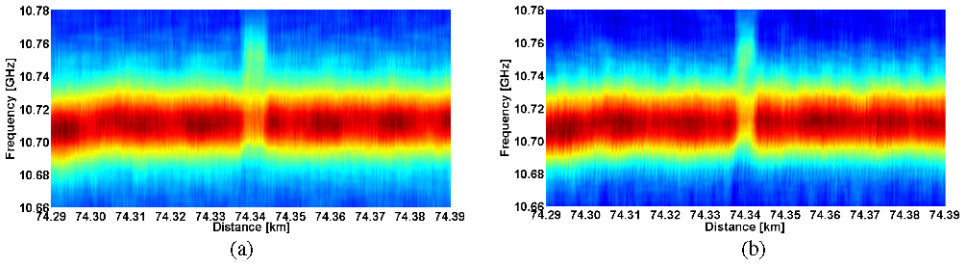

Fig. 4. Brillouin gain sweep around the hot spot (located around km 74.34). The probe signal frequency is swept from 10.66 GHz until 10.78 GHz with (a) 65 ns pulses and (b) 55 ns pulses. The traces are not de-noised, therefore periodic noise is visible at some positions.

The result of the subtraction of these two traces is shown in Fig. 5(a). A 1 meter hot-spot is clearly visible, in km 74.343. The maximum gain clearly switches from the value of 10.71 to 10.76. This frequency difference can be easily translated to temperature by using the sensitivity of the BFS to temperature, which is 1.3 MHz/°C in our particular case [9], [14]. Therefore, the 50 MHz frequency difference in the hot spot could be translated as 38°C difference, which actually matches with the expected temperature change. In Fig. 5(b) the same gain sweep is observed without the de-noising procedure applied. It can be clearly seen that the contrast of the resulting gain trace sweep is degraded, showing the efficiency of the

#165389 - $15.00 USD Received 23 Mar 2012; revised 27 Apr 2012; accepted 28 Apr 2012; published 14 May 2012

developed procedure. Figure 5(c) shows the gain sweep at the exact position of the hot-spot. It is noticeable a gain increase at the hot-spot frequency (~10.76 GHz) and a good extinction at the position of the maximum of the rest of the fiber (~10.71 GHz). Lastly, Fig. 5(d) displays the representation of the BFS (υ_B) with and without the de-noising procedure. The rms frequency difference between consecutive traces is in the order of 3 MHz, when the de-noising is used (5 MHz without de-noising), which ensures a maximum uncertainty of ~2.3°C in the measurement of the hot-spot (3.8°C without using de-noising). Our simple de-noising procedure thus helps to reduce ~1.5 °C in uncertainty.

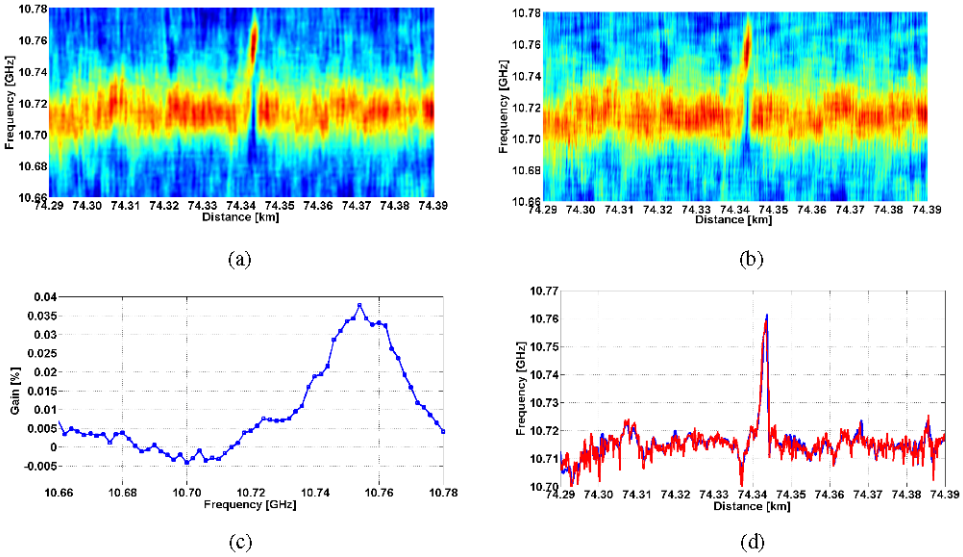

Fig. 5. Result of the subtraction between the 65 ns and 55 ns Brillouin gain traces for the 1 meter hot-spot (a) with the de-noising procedure and (b) without the de-noising procedure (100 meter span); (c) gain profile obtained at the position of the hot-spot; (d) BFS representation with and without the de-noising procedure (blue and red traces respectively).

In a second experiment, we attempted to perform sub-metrical resolution measurements employing exactly the same setup as depicted in Fig. 1. We introduced 0.8 meter fiber in the hot bath and measured with 65 ns and 57 ns pulses, where the 8 ns pulse-width difference should provide 0.8 meter resolution. Figure 6(a) shows the result of the subtraction of both traces (50 m span measurement) with the de-noising procedure applied. As it can be seen, the 0.8 meter hot-spot is perfectly detectable at the expected frequency position (10.76 GHz). Figure 6(b) shows the gain sweep at the exact position of the hot-spot. Once again, it is noticeable a gain increase at the hot-spot frequency (~10.76 GHz) and almost a complete absence of gain at the position of the un-shifted maximum (~10.71 GHz). These results show that the spectral purity issues associated to imperfect extinction ratio in the pulses [12] are not evident in this experimental configuration. Figure 6(c) represents the BFS of the subtraction and in this case, compared to the case of 1 meter resolution, the rms frequency difference between consecutive sweeps is in the order of 6 MHz, slightly higher than before, which determines an rms uncertainty in the measurement of roughly 4.6°C.

#165389 - $15.00 USD Received 23 Mar 2012; revised 27 Apr 2012; accepted 28 Apr 2012; published 14 May 2012

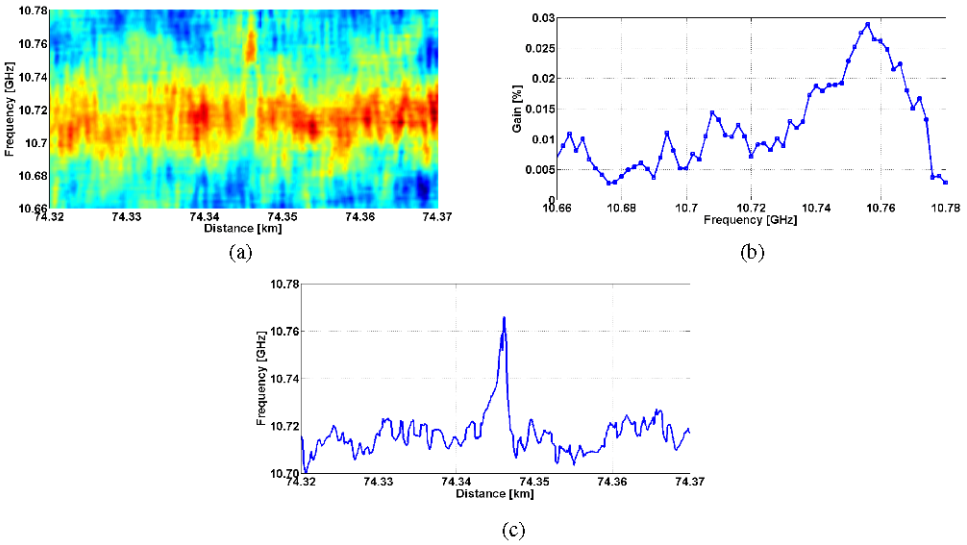

Fig. 6. (a) Result of the subtraction between the 65 ns and 57 ns Brillouin gain traces for the 0.8 meter hot-spot with the de-noising procedure (50 meter span); (b) gain profile obtained at the position of the hot-spot; (c) BFS representation.

4. Further improvement using a semiconductor pump in the probe end

By comparing the results for 1 meter and for 0.8 meter resolution, it is noticeable a considerable decrease in the quality of the measurement in terms of noise, even when the de-noising procedure is applied. This noise problem becomes certainly impossible to handle at lower resolution values with this experimental arrangement. This is due to the simultaneous occurrence of two problems: first, the detection bandwidth has to be correspondingly increased, which implies an equivalent increase in noise bandwidth; second, the energy of the trace difference becomes smaller. To push further down the resolution, we decided to use Semiconductor Laser (SL) pumping on the probe side of our BOTDA. This type of lasers has much lower RIN values than RFLs (typically −105 dBc/Hz for RFLs and −140 dBc/Hz for SLs). Their positive use in BOTDA was successfully confirmed by Soto et al. in previous works [10]. The choice of SL pumping in the probe end minimizes the RIN transfer issues in detection. Detailed analysis of RIN transfer issues can be found in [9–10].

As it was done in the previous experiments, in this case 0.5 meter fiber length was introduced in the hot bath and two measurements were developed with 65 and 60 ns pulse widths. The pumping in the probe end is done at similar power levels than in the previous case (~230 mW), except for the fact that the SL is providing the pump entering through the probe end. The Raman pump on the other side is left unaltered. In Fig. 7(a) (100 m span measurement) it can be seen the subtraction between the obtained traces and once the de-noising procedure is applied. It is noticeable that the detection of the hot-spot is performed properly and that in this position (~74.34 km) the gain completely switches from 10.71 GHz to 10.76 GHz. The measurement quality is clearly better than the case of 0.8 meter explained above. Figure 7(b) shows the gain sweep at the exact position of the hot-spot. Compared with the results obtained for 0.8 meter resolution (Fig. 6(b)), it is remarkable the improvement achieved by introducing the semiconductor pump, especially when sensing at the hot-spot region. In Fig. 7(c) we depict the obtained BFS curve. By subtracting consecutive traces we could determine that the rms uncertainty of the measurement is close to 2.9°C (3.8 MHz). This frequency uncertainty is essentially affected by three parameters: the trace noise (whose main cause is still RIN transfer due to Raman amplification), the frequency step in our measurement (2 MHz), and the gain bandwidth (which is ~30 MHz in this case). The main route to improve the measurements could be the reduction of trace noise (through trace

#165389 - $15.00 USD Received 23 Mar 2012; revised 27 Apr 2012; accepted 28 Apr 2012; published 14 May 2012

averaging or coding techniques) or reducing the frequency step in the sweep. Coding would be the preferred option, since the other options would also imply a corresponding increase in measurement time.

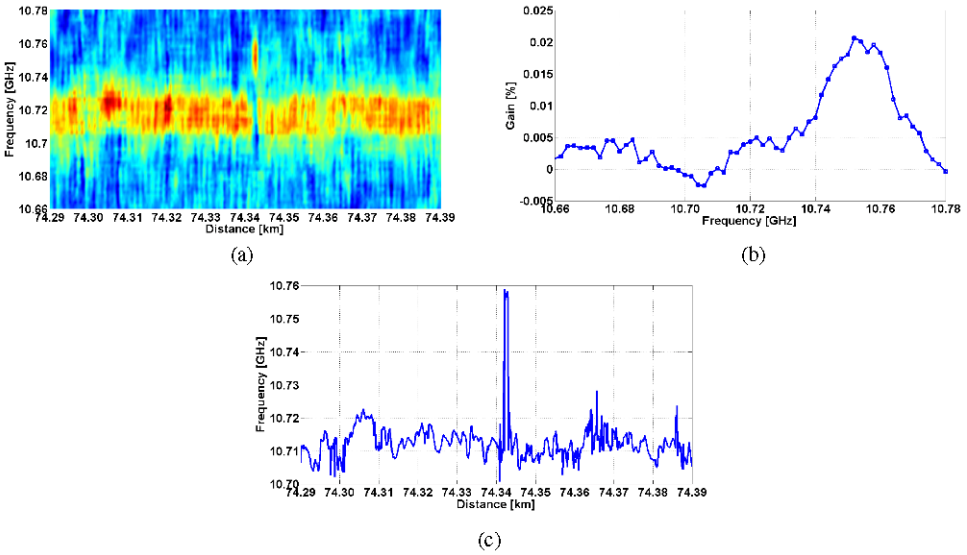

Fig. 7. (a) Result of the subtraction between the 65 ns and 60 ns Brillouin gain traces for the 0.5 meter hot-spot with the de-noising procedure (100 meter span); (b) gain profile obtained at the position of the hot-spot; (c) BFS representation.

5. Conclusion

In this work we have presented a high resolution long-range Raman-assisted BOTDA temperature sensor based on the DPP technique that resolves in a distributed way sub-meter hot-spots all along 100 km. This has been achieved by a careful engineering of the sensing setup and a novel de-noising procedure that minimizes the RIN transfer issue in Raman-assisted configurations, in the usual case of pumping with a fiber laser.

1, 0.8 and 0.5 meter hot-spots are clearly detected with good contrast, the latter using semiconductor laser-based Raman pumping in the probe end. In this case, the estimated rms uncertainty in the measurements is in the order of 2.9°C. The results achieved illustrate that this technique has potential to provide good results in the sub-meter range, especially when the Raman assistance in the setup is done with semiconductor lasers.

Acknowledgments

This work was supported in part by the Spanish Ministry of Science and Innovation through projects TEC2009-14423-C02-01 and TEC2009-14423-C02-02 and the Comunidad de Madrid through project FACTOTEM-2. Sonia Martin-Lopez acknowledges funding from the Spanish Ministry of Science and Innovation through a “Juan de la Cierva” contract. We also acknowledge discussions with Dr. Juan Diego Ania-Castañon (CSIC) and Prof. Luc Thévenaz (EPFL, Switzerland).